

Relevance of phonon dynamics in strongly correlated systems coupled to phonons: A Dynamical Mean Field Theory analysis

Giorgio Sangiovanni¹, Massimo Capone^{2,3} and Claudio Castellani²

¹ *Max-Planck Institut für Festkörperforschung, Heisenbergstr. 1, D-70569 Stuttgart, Germany*

² *Istituto dei Sistemi Complessi, Consiglio Nazionale delle Ricerche, Via dei Taurini 19, I-00185 Roma, Italy*

³ *CNR-INFM Statistical Mechanics and Complexity Center, and Dipartimento di Fisica
Università di Roma "La Sapienza" piazzale Aldo Moro 5, I-00185 Roma, Italy*

(Dated: December 28, 2021)

The properties of the electron-phonon interaction in the presence of a sizable electronic repulsion at finite doping are studied by investigating the metallic phase of the Hubbard-Holstein model with Dynamical Mean Field Theory. Analyzing the quasiparticle weight at finite doping, we find that a large Coulomb repulsion reduces the effect of electron-phonon coupling at low-energy, while this reduction is not present at high energy. The renormalization of the electron-phonon coupling induced by the Hubbard repulsion depends in a surprisingly strong and non-trivial way on the phonon frequency. Our results suggest that phonon might affect differently high-energy and low-energy properties and this, together with the effect of phonon dynamics, should be carefully taken into account when the effects of the electron-phonon interaction in a strongly correlated system, like the superconducting cuprates, are discussed.

PACS numbers: 71.27.+a, 71.10.Fd, 71.30.+h, 71.38.-k

I. INTRODUCTION

One of the open problems of high-temperature superconducting cuprates is the role played by the electron-phonon interaction. The experimental evidences suggest a fairly strong influence of the electron-phonon interaction on some physical properties, while for some other aspects, lattice effects seem to have almost no role. On one side, inelastic scattering measurements have shown that a specific optical in-plane phonon mode displays an anomalously pronounced softening.^{1,2,3,4} The coupling to the same phonon mode has been invoked to explain the kink in the nodal electron dispersion detected by photoemission,^{5,6,7} On the other hand, the almost perfectly linear behavior of the resistivity in a wide range of temperatures seems to indicate a little influence of phonons on transport properties. Isotope effects also show a complex phenomenology: While the superconducting temperature has a little isotope effect at optimal doping,^{8,9,10} the in-plane penetration depth is much more sensitive to isotope substitution.^{11,12,13} Such a large (around 5%) effect is usually translated into an isotope effect on the effective mass suggesting the presence of polaronic carriers in underdoped compounds.¹⁴

The above puzzling scenario leads to a lively debate which ultimately focuses on whether the effects of electron-phonon (e-ph) coupling on different quantities are depressed or enhanced by the presence of strong correlations. Given the intrinsic nonperturbative character of the problem, there is no obvious theoretical approach. Different approaches seem indeed to draw conflicting scenarios in studies of the Holstein model for the e-ph coupling in the presence of strong correlations, described by the Hubbard or the t - J models. According to Quantum Monte Carlo (QMC) and exact diagonalization (ED) a single hole in the t - J model expe-

riences an enhanced polaronic effect due to the “pre-localizing” mechanism associated to the antiferromagnetic spin background.^{15,16,17,18} QMC calculations in the Hubbard model at finite density and fairly high temperature suggest that strong correlations favor the small transferred momentum electron-phonon vertex (or depress it less than its large momentum counterpart), and that this quantity increases by increasing repulsion for a window of parameters.¹⁹ Slave boson approaches suggest however that such an effect is just a finite-temperature precursor of a phase separation that would take place at low temperatures.^{20,21} Such tendency towards phase separation, indicated by mean-field approaches also for the three-band Hubbard model,²² has been recently confirmed by the more accurate Dynamical Mean Field Theory (DMFT).²³

Another piece of information comes from the DMFT of the half-filled Hubbard-Holstein model in the paramagnetic sector (i.e., neglecting the antiferromagnetic ordering), where detailed phase diagrams are available.^{24,25} In Ref. 26 we have shown that, close to the Mott transition, phonons have different effects on high- and low-energy single particle properties (self-energy, spectral weights, density of states, ...). Namely, high-energy features are significantly affected by phonons, whereas the low-energy quasiparticle features are basically untouched and they coincide with those of an effective purely electronic with a slightly weaker repulsion U . In other words, the strong correlations strongly reduce the impact of e-ph interaction on quasiparticle properties, at least when the e-ph coupling is not too large. The only residual effect is a phonon-induced screening of U which moreover is found to vanish linearly with the phonon frequency in the adiabatic limit.

This variety of results is certainly due to the different physical regimes they refer to. In this work we start from

our analysis of the half-filled Hubbard-Holstein model and relax the half-filling condition, therefore putting ourselves away from the Mott transition, in a regime closer to that of other approaches. We find that strong correlations still significantly harm the e-ph interaction. In our strongly correlated metal polaronic behavior only establishes for e-ph coupling larger by at least a factor two than the corresponding values in the absence of strong correlations or for a single hole in an antiferromagnetic background. Moreover, we find that the interplay of electron-electron and e-ph interaction makes the value of the phonon frequency quite relevant, particularly for its effect on the effective mass. Remarkably, phonon dynamics turns out to be more relevant close to half-filling.

The paper is organized as follows: in sec. II we compare the half-filled and finite doping cases of the Hubbard-Holstein model. In sec. III we analyze the renormalization of the quasiparticle weight as a function of the electron-phonon coupling and the phonon frequency. In sec. IV the behavior of the chemical potential is studied and the conclusions are then drawn in sec. V.

II. DMFT OF THE HUBBARD-HOLSTEIN MODEL: HALF-FILLING VS FINITE DOPING

The Hamiltonian of the Hubbard-Holstein model reads

$$H = -t \sum_{\langle i,j \rangle, \sigma} c_{i,\sigma}^\dagger c_{j,\sigma} + U \sum_i n_{i\uparrow} n_{i\downarrow} - g \sum_i n_i (a_i + a_i^\dagger) + \omega_0 \sum_i a_i^\dagger a_i, \quad (1)$$

where $c_{i,\sigma}$ ($c_{i,\sigma}^\dagger$) and a_i (a_i^\dagger) are, respectively, destruction (creation) operators for fermions with spin σ and for local vibrations of frequency ω_0 on site i , t is the hopping amplitude, U is the local Hubbard repulsion and g is an electron-phonon coupling constant. In this work we will always consider an infinite coordination Bethe-lattice with semicircular density of states of semibandwidth D . $\lambda = 2g^2/\omega_0 D$ is the standard electron-phonon coupling and ω_0/D is the adiabatic ratio.

We solve the model by means of Dynamical Mean-Field Theory (DMFT), which in recent years has emerged as one of the most reliable tools for the analysis of both correlated materials and electron-phonon interactions. The method maps the lattice model onto an effective local theory which still retains full quantum dynamics, and it is therefore expected to be quite accurate for models with local interactions as (1). The mean-field correspondence between the local theory and the original model is achieved by imposing a self-consistency condition which contains the information about the original lattice.²⁷ In practice, the local problem is described through an Anderson-Holstein impurity model,^{28,29} whose impurity Green's function has to be calculated and used to generate a new impurity model through the self-consistency equation. To solve the impurity model we use ED,³⁰ truncating the infinite phonon Hilbert space allowing up

to N_{max} phonon states (ranging from 20 to 40), and using up to $N_b = 9$ sites in the conduction bath.³¹

DMFT has been widely used to study the properties of the Hubbard model, and a clear framework for the Mott-Hubbard transition has been determined. Without entering the details of these studies, we just recall the qualitative difference between the half-filled system, where a metal-insulator occurs at $U = U_{c2} \simeq 3D$, and finite-doping systems that have metallic character regardless the value of U . Such a distinction makes the effects of phonons different in the two cases.

At half-filling, in the strongly correlated metallic phase for U smaller, but not far from U_{c2} , the Hubbard model presents a clear separation of energy scales, with high-energy Hubbard bands well separated from the low-energy quasiparticle peak. In this regime the charge fluctuations are frozen, therefore strongly harming the e-ph interaction, at least with a Holstein coupling. As discussed in Ref. 26, the residual effect of phonons can be described as a partial screening of the static Hubbard repulsion, which is ruled by the parameter ω_0/U , according to the expression $U_{eff} = U - \eta\lambda D$, with η given by

$$\eta = \frac{2\omega_0/U}{1 + 2\omega_0/U}. \quad (2)$$

Notice that the above expression for U_{eff} correctly reproduces the antiadiabatic limit $\omega_0/D \rightarrow \infty$, where the e-ph interaction mediates an instantaneous local attraction of strength λ . The description in terms of an effective Hubbard model with a suitably rescaled repulsion U_{eff} works surprisingly well in the proximity of the Mott transition: The full Hubbard-Holstein model and the effective purely electronic model display an identical electronic spectrum at low energy and, quite remarkably, the same rescaling for U_{eff} makes the position of the Hubbard bands basically coincide. The effects of the electron-phonon coupling close to the Mott transition are well visible in the high-energy parts of the electronic spectrum, where phonon satellites show up, while the low-energy metallic peak turns out to be “protected” by correlation.

This paper is devoted to the extension of this analysis to generic fillings, still limiting ourselves to the paramagnetic sector. Conceptually the peculiarity of half-filling is the clear separation between high- and low-energy scales, which is rapidly lost as the density deviates from one. This lack of hierarchy of energy scales makes it more complicated to draw a simple physical picture such as the one described above. On the other hand, the properties of the metallic phase at finite doping are not severely affected by the antiferromagnetic order, which, if included, would instead change considerably the half-filling picture.

III. QUASIPARTICLE PROPERTIES

As in Ref. 26, we start our analysis from the inspection of the quasiparticle weight

$$Z = \left(1 - \frac{\partial \Sigma'(\omega)}{\partial \omega} \Big|_{\omega=0} \right)^{-1} \quad (3)$$

where Σ' is the real part of the local self-energy Σ . Due to the momentum independence of the self-energy in DMFT, Z is also inversely proportional to the quasiparticle effective mass ratio m^*/m . It is therefore clear that this quantity measures the metallic nature of the system, small values of Z implying poorly metallic situations.

A. Dependence on electron-phonon coupling

At half-filling, in the correlated metal for $U \lesssim U_{c2}$, the quasiparticle weight Z *increases* with the electron-phonon coupling λ .^{25,26} This counterintuitive behavior, in stark contrast with weakly correlated systems, where Z decreases with λ , is understood in terms of a phonon-driven attraction which counteracts the Hubbard repulsion, and it can be quantitatively described within the effective picture introduced in sec. II:²⁶ By increasing λ , the effective repulsion decreases, thus the system becomes less correlated, and the value of Z increases. As mentioned above, such a reduced effectiveness of the e-ph coupling can be associated to the freezing of charge fluctuations, to which the phonons are coupled. Close to Mott state, most sites are singly occupied, and doubly occupied and empty sites are a minority. As soon as we move away from half-filling, doping, e.g., with holes, the number of empty sites proliferates. Therefore charge fluctuations are gradually restored, even if they are still reduced with respect to a system without electron correlations. As a consequence, one can expect a stronger electron-phonon signature with respect to half-filling. The behavior of Z rapidly becomes more ordinary, namely Z decreases as a function of λ (except, as we will see below, for extremely large ω_0 of the order of U) meaning that the predominant effect of the coupling to the lattice is of localizing nature.

This is also consistent with a much weaker dependence of Z on U for $U \simeq 5D$ (in comparison with the case $U \simeq U_c$ at half-filling) which would depress the delocalizing effect of any phonon-induced variation of U into U_{eff} .

In Fig. 1 we plot m^*/m as a function of λ for different doping levels and for $\omega_0 = 0.2D$. In the left panel we show the uncorrelated system ($U = 0$). m^*/m is equal to 1 for $\lambda = 0$, it rapidly increases with λ , eventually reaching a polaronic regime, testified by an exponential growth of the effective mass and by the development of finite lattice distortions coupled to the electrons.³² The right-hand panel presents instead a strongly correlated case ($U = 5D$). Here the value of m^*/m at $\lambda = 0$ is strongly dependent on density, since correlations are

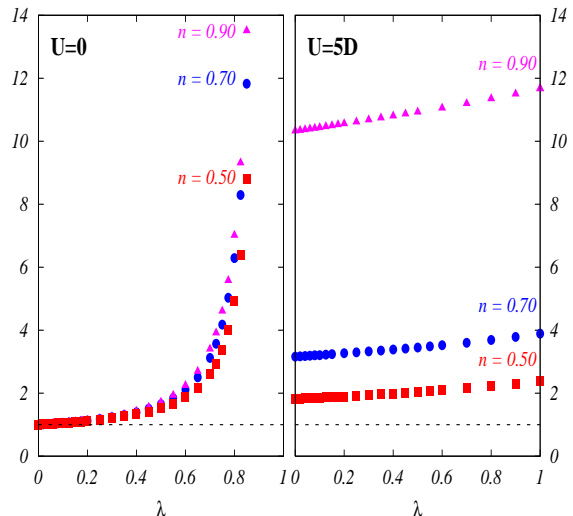


FIG. 1: (Color online) Calculated values of m^*/m as a function of λ for various values of the density. In both cases of $U = 0$ (left) and $U = 5D$ (right) the phonon frequency ω_0 has been fixed to $0.2D$.

more and more effective in localizing the carriers the closer we are to half-filling. In practice $m^*/m \simeq 2$ already for $n = 0.50$ and it reaches more than 10 for $n = 0.9$. The main result is however that the e-ph interaction is not able to substantially modify this values determined by correlation, up to $\lambda = 1.0-1.5$ and m^*/m is almost flat in this interval, if compared with the left panel. Thus, even if doped system do not show the growth of Z with λ characteristic of half-filling (close to U_{c2}), the effect of e-ph coupling is anyway quantitatively reduced by a sizable amount. A similar information is brought by the location of the polaron crossover: If we consider larger value of λ than in Fig. 1, the e-ph interaction finally becomes able to sizably affect the quasiparticle residue Z . In the example shown in Fig. 2 ($U = 5D$, $n = 0.9$, $\omega_0/D = 0.2$), the curve of Z as a function of λ clearly displays a crossover between a small- λ linear behavior and a much faster decrease for $\lambda \gtrsim 2 \div 2.5$. This is precisely the signature of a polaron crossover, as shown by many studies for the pure Holstein model, where a similar bending of the curve occurs for much smaller $\lambda \simeq 0.8$.^{32,33}

An alternative marker of the polaron crossover is the phonon displacement distribution $P(X) = \langle \psi_0 | X \rangle \langle X | \psi_0 \rangle$, where $|\psi_0\rangle$ is the groundstate vector, and $|X\rangle\langle X|$ is the projection operator on the subspace where the phonon displacement value $\hat{X} = 1/\sqrt{2M\omega_0}(a + a^\dagger)$ (M being the phonon mass) has a given value X . This quantity therefore measures the distribution of the local distortions. At weak coupling, $P(X)$ has only one peak, which only broadens when the coupling increases, but when a polaronic groundstate is realized, it presents two peaks, corresponding to different distortions associated to the different charge states.³⁴ The two insets of Fig.

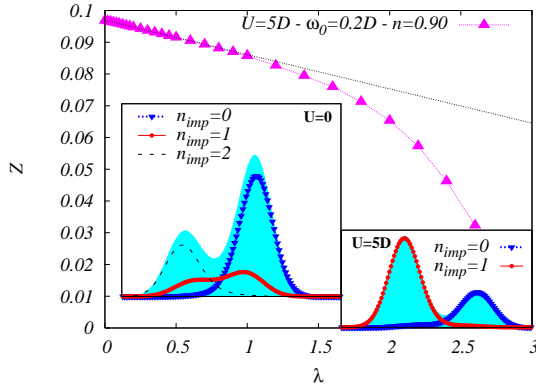


FIG. 2: (Color online) Behavior of the quasiparticle weight Z (main panel) in the crossover from weak to strong λ for $U = 5D$, $n = 0.90$ and $\omega_0 = 0.2D$. In the two insets the phonon distribution function $P(X)$ in the polaron region are shown for $U = 5D$ (smaller inset, $\lambda = 2.8$) and $U = 0$ (larger one, $\lambda = 0.875$). In both insets $n = 0.70$ and $\omega_0 = 0.2D$. The light blue shaded area is the full $P(X)$ while the triangles, solid circles and dashes represent $P(X)$ restricted to $n_{imp} = 0, 1$ and 2 respectively.

2 show $P(X)$ for two sets of parameter chosen in order to highlight the different way to realize the bimodality in the uncorrelated system (left/larger panel) and in the strongly correlated one (right/small panel). The simple $P(X)$, shown as a shaded area, does not allow us to distinguish the two situations. Therefore we also plot the conditioned probability distributions projected onto the states in which the impurity has different occupations $n_{imp} = 0, 1, 2$.²⁸ For $U = 0$ the bimodality is associated to a large number of empty and doubly occupied sites (that gain more e-ph energy), and a smaller number of singly occupied ones. This is a signature of bipolaronic groundstate, where pairs of polarons are formed. Since we are at finite doping the two distributions have different shapes and heights. For $U = 5D$ the two peaks of $P(X)$ are instead associated to empty sites and singly occupied ones, since the strong on-site repulsion unfavors double occupancies. Exploiting the empty sites, the system can acquire polaronic groundstate at intermediate values of λ , while at half-filling this would require to completely overcome the Hubbard U . We finally notice that in the special half-filling case $P(X)$ is not the ideal quantity to identify the polaronic behavior, which, at intermediate values of λ , can only appear in the dynamics of the excitations (e.g. the behavior of a single hole)

To summarize the results of this section, we can conclude that for metallic situations with finite doping it is not possible to describe the effects of the phonons on quasiparticle properties in terms of an effective screened Coulomb repulsion, as it happened at half-filling. It is anyway still true that the effect of phonons on quasiparticle properties is substantially weaker than for weakly correlated systems, and that the phonon effects can be

strong only in the high-energy part of the spectra.³⁵ The polaron crossover is found at values of λ which are sensibly larger than in the absence of strong correlation.

B. Dependence on phonon frequency

As it has been discussed in many previous studies, the coupling λ is not the only parameter which controls the properties of e-ph interaction, since also the phonon frequency plays an important role.^{36,37,38} In this section we investigate precisely the role of this quantity in strongly correlated systems.

In Fig. 3 we report Z as a function of λ , for $U = 5D$, $n = 0.70$ and different values of ω_0 . The antiadiabatic curve (denoted by $\omega_0 = \infty$) is simply obtained for a Hubbard model with total repulsion given by $U - \lambda D$. In the region $\lambda \lesssim 1$, well before any polaronic behav-

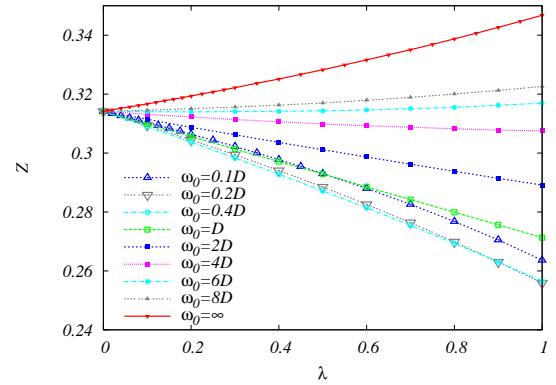


FIG. 3: (Color online) Quasiparticle weight Z as a function of λ for different values of ω_0/D . $U = 5D$ and $n = 0.70$.

ior, Z is almost linear in λ , with a slope strongly dependent on ω_0 . In Fig.4 we plot the slope r , defined through $Z/Z_{\lambda=0} = 1 + r\lambda$. For $\omega_0 \rightarrow \infty$, where the phonons only give rise to an instantaneous attraction, which opposes the Hubbard repulsion, Z increases as a function of λ , and $r > 0$. This behavior is indeed limited to $\omega_0 > 5D$, while for smaller frequencies the phonons play a more standard role, decreasing Z , as expressed by a negative r . More interestingly, r displays a non-monotonic behavior by further decreasing ω_0 . Starting from $\omega_0 = 0$, it decreases up to $\omega_0 \simeq 0.3D$, roughly independently on doping, and then rises, remaining negative for a wide range of frequencies, and eventually becoming positive for quite large ω_0/D . While the evolution of r from negative to positive can be simply understood in terms of a crossover from an adiabatic region, where λ acts as a localizing force, to an antiadiabatic one where λ decreases the localizing power of U , the non-monotonic behavior suggests that the strongly correlated systems displays more relevant energy scales. The same phenomenon can be observed by plotting the effective mass

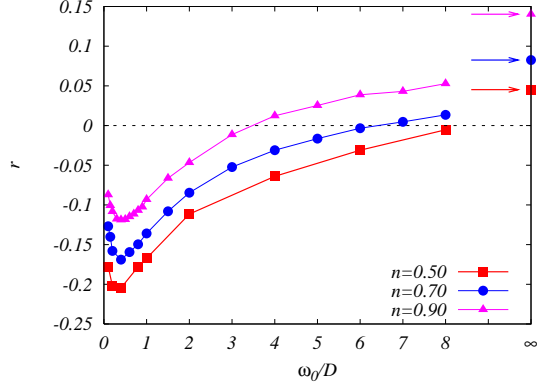


FIG. 4: (Color online) Coefficient r , defined as the slope of $Z/Z_{\lambda=0}$ for small λ as a function of ω_0/D , for $n = 0.50, 0.70$ and 0.90 .

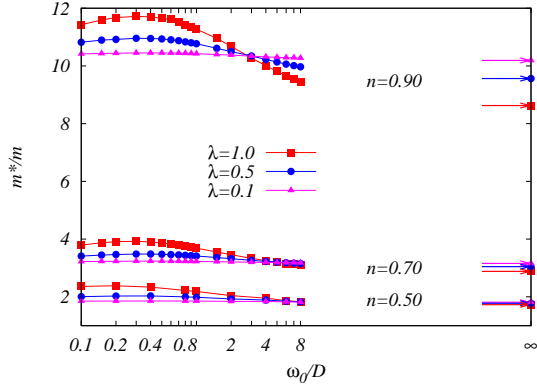


FIG. 5: (Color online) Quasiparticle effective mass vs. ω_0 for $\lambda = 0.1, 0.5$ and 1.0 , at $U = 5D$ in a semi-logarithmic plot. The three cases $n = 0.50, 0.70$ and 0.90 are shown on the same scale.

m^*/m as a function of ω_0 at fixed λ , as we do in Fig. 5 for the same three values of the doping. The derivative of this curve is a measure of the isotope coefficient on the effective mass α_{m^*} . For pure e-ph systems m^* always decreases with ω_0 at fixed λ : In the adiabatic regime it initially decreases linearly with ω_0 while, for $\omega_0 \gg D$, it scales as $1/\omega_0$.³⁹ Therefore the isotope coefficient $\alpha_{m^*} = \frac{1}{2} \frac{\partial \log(m^*/m)}{\partial \log(\omega_0/D)}$ is always negative. We find instead that, in the presence of strong correlation, m^* can increase as a function of ω_0 . This effect is larger for densities close to the density-driven metal-insulator transition: For instance, for $n = 0.90$, the value of α_{m^*} for $\omega_0 \simeq 0.1D$ and $\lambda \simeq 1.0$ is a positive, even if quite small, number $\alpha_{m^*} \simeq 1 \div 2 \times 10^{-2}$. For values of ω_0 around $0.3D$ the effective mass becomes instead almost independent on the phonon frequency, then α_{m^*} changes sign and m^*/m monotonically approaches the asymptotic antiadiabatic value. These results have an interesting consequence on the interpretation of the experiments on

strongly correlated materials: The sign and the magnitude of α_{m^*} is very sensitive to the values of the electron-phonon coupling and of the phonon frequency of the specific compound.^{39,40} Furthermore, a small value of α_{m^*} can be observed if a compound is in the crossover region between the two regimes, but this cannot be interpreted as a sign of applicability of the Migdal-Eliashberg theory, despite this latter predicts indeed $\alpha_{m^*} = 0$. Turning to the cuprates, the sizable ($\alpha_{m^*} \sim -0.5$) negative isotopic effect for the effective mass extracted from the isotopic dependence of the penetration depth,¹⁴ would suggest quite larger values of λ than those studied here, putting these materials near (or beyond) the polaronic instability. It is well possible that the antiferromagnetic correlations, neglected in this paper, favor a polaronic behavior at least by decreasing doping. Indeed the experimental evidences for a polaronic behavior in the cuprates are limited to extremely small doping, well inside the antiferromagnetic phase.⁴¹

The isotope effect has instead a different behavior at half-filling for $U \lesssim U_{c2}$. Close to the Mott-Hubbard transition m^* decreases with ω_0 , but the absolute value of α_{m^*} is extremely large.^{26,42} This can be explained once more by the effective-Hubbard picture with $U_{eff} = U - \eta\lambda D$ and $\eta = 2\omega_0/U$ valid at half-filling and for $U \lesssim U_{c2}$: close to the Mott-Hubbard transition, in fact, DMFT predicts that, for a pure Hubbard model with $U = U_{eff}$, $m^* \propto U_{c2}/(U_{c2} - U_{eff})$ i.e.

$$m^* \propto \frac{U_{c2}}{U_{c2} - U + 2\omega_0\lambda D/U} \quad (4)$$

An increase in the phonon frequency ω_0 at fixed λ determines then a sizable decrease in the effective mass. The final result is $\alpha_{m^*} \propto -1/Z$, in other words the absolute value of α_{m^*} gets larger and larger, the closer one gets to the Mott transition.

Finally we notice that the bare value of r obtained in the absence of correlations does not depend strongly on the phonon frequency up to $\omega_0 \sim D$. In the adiabatic limit by $r_0 = -N(E_F)$, where $N(E_F)$ is the non interacting density of states at the Fermi energy. For a semicircular density of states and $n \simeq 0.5 \div 1$, one gets $r_0 \simeq -0.58 \div 0.64$. Comparing with Fig. 4, it turns out that this bare value is larger by a factor $2 \div 6$ than the corresponding maximum values in the interacting case. If we define an effective coupling for the quasiparticles according to $1 + r\lambda \equiv 1 + r_0\lambda_{eff}$, we see that λ_{eff} is rather smaller than λ and this reduction is unusually enhanced at small frequency (r_0 will instead be maximum at $\omega_0 = 0$). At the same time, as discussed in sec. III, the polaronic crossover is pushed to higher values of λ .

C. Fermi-liquid theory vs DMFT

One of the main results of the previous analysis is that strong correlation tends to reduce the effects of e-ph interaction, and the size of this effect depends on the

phonon frequency. An important question is whether or not the behavior of the quasiparticle weight Z obtained in DMFT in the metallic region away from polaronic instabilities can be captured, at least qualitatively, by a weak coupling approach to the interaction between quasiparticles and phonons. In particular we can test the validity of a Fermi-liquid analysis in which a clear hierarchy is supposed: electron-electron correlations create heavy quasiparticles, which in turn interact with the phonons via a renormalized density vertex. It is understood that DMFT is not able to deal with the momentum dependence of the renormalized vertex.

We divide the self-energy in two contributions:

$$\Sigma(\mathbf{k}, \omega) = \Sigma_{\lambda=0}(\mathbf{k}, \omega) + \Sigma_{res}(\mathbf{k}, \omega) \quad (5)$$

where $\Sigma_{\lambda=0}$ is the self-energy of the pure Hubbard model, and Σ_{res} contains all the additional interaction due to bare and correlation-dressed electron-phonon processes. We can define a quasiparticle residue $Z_{\lambda=0}$ determined only by electronic correlations (We recall that Σ' is the real part of Σ .)

$$Z_{\lambda=0} = \left(1 - \left. \frac{\partial \Sigma'_{\lambda=0}(\mathbf{k}, \omega)}{\partial \omega} \right|_{\omega=0} \right)^{-1} \quad (6)$$

which is related to the full quasiparticle weight Z by

$$\frac{Z}{Z_{\lambda=0}} = \left(1 - Z_{\lambda=0} \left. \frac{\partial \Sigma'_{res}(\mathbf{k}, \omega)}{\partial \omega} \right|_{\omega=0} \right)^{-1}. \quad (7)$$

$Z/Z_{\lambda=0}$ may be seen as a wave-function renormalization for the quasiparticles created by U due to the additional interaction, and the quantity $Z_{\lambda=0} \Sigma'_{res}$ plays the role of a phonon-induced self-energy for those quasiparticles.

In the small- λ regime, and assuming that the quasiparticle self-energy is linear in ω , Eq. (7) can be written as

$$Z^{qp} = \frac{Z}{Z_{\lambda=0}} = 1 + r\lambda, \quad (8)$$

where r coincides with the phenomenological parameter introduced in sec. IIIB and plotted in Fig. 4. Within Fermi-liquid theory we can derive an expression for r at the lowest order in λ assuming that Σ_{res} only contains e-ph processes dressed by U :

$$Z_{\lambda=0} \frac{\partial \Sigma'_{res}}{\partial \omega} = -N(E_F)^* V^* \Lambda^2 = -N(E_F) Z_{\lambda=0} \Lambda^2 \lambda D \quad (9)$$

where $N(E_F)^* = N(E_F)/Z_{\lambda=0}$ is the quasiparticle density of states, $V^* = \lambda D Z_{\lambda=0}^2$ is the renormalized e-ph interaction between quasiparticles, and Λ is the vertex which couples the electrons to the phonons (a density vertex for the Holstein model). Eq. (9) obviously implies $r = -Z_{\lambda=0} \Lambda^2 N(E_F)$. This result holds as long as

one considers only those self-energy diagrams in which correlation dresses exclusively the vertex.

There are only two specific limiting cases in which, making use of Ward Identities,^{22,43} we are able to find explicit expressions for the density vertex Λ : the static and the dynamic limit. These read respectively

$$Z_{\lambda=0} \Lambda(q \rightarrow 0, \omega = 0) = \frac{1}{1 + F_0^{s(e)}}, \quad (10)$$

and

$$Z_{\lambda=0} \Lambda(q = 0, \omega \rightarrow 0) = 1 \quad (11)$$

where $F_0^{s(e)}$ is the symmetric Landau scattering amplitude due to electronic processes. Since we are considering electronic processes only, we have, in the static limit $\Lambda = \kappa^{(e)}/\kappa_0^{(e)}$ where $\kappa^{(e)}$ is the compressibility of the Fermi liquid in the absence of coupling to the lattice, while $\kappa_0^{(e)}$ is the non-interacting value equal to $2N(E_F)$. Then Eq. (9) can be written, in the static limit, as

$$Z_{\lambda=0} \frac{\partial \Sigma'_{res}}{\partial \omega} = -N(E_F) Z_{\lambda=0} \left[\frac{\kappa^{(e)}}{\kappa_0^{(e)}} \right]^2 \lambda D \quad (12)$$

In the opposite dynamic limit, instead, $\Lambda = 1/Z_{\lambda=0}$ and Eq. (9) becomes

$$Z_{\lambda=0} \frac{\partial \Sigma'_{res}}{\partial \omega} = -\frac{N(E_F)}{Z_{\lambda=0}} \lambda D \quad (13)$$

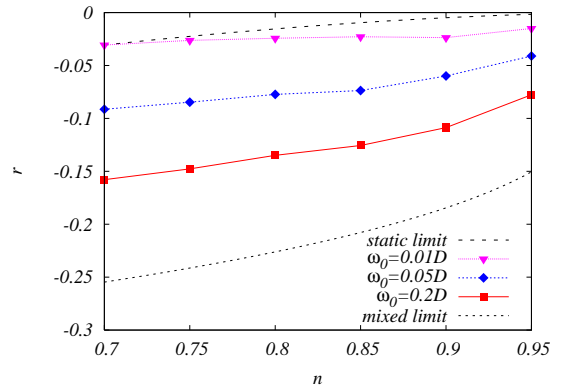


FIG. 6: Coefficient r as a function of the density for three small values of ω_0/D . The meaning of the curves labeled as static and mixed limit is described in the text.

We are now in the position to compare the above Fermi-liquid analysis with the DMFT results, where all the contributions to the electronic self-energy are considered. In particular we focus on the small- ω_0 regime, where the interplay between attraction and repulsion is more subtle, as suggested by the data of Fig. 4. In Fig. 6 we report the coefficient r , for $\omega_0/D = 0.2$ and for two smaller values and compare them, in the range of

densities between 0.7 and 0.95 to the static limit result $r = -N(E_F)Z_{\lambda=0}(\kappa^{(e)}/\kappa_0^{(e)})^2$ of Eq. (12). The dynamic limit (13) is not shown because it gives $r \propto -1/Z_{\lambda=0}$, thus divergent in the limit $n \rightarrow 1$. This is evidently not comparable with the DMFT results shown in Fig. 6, implying that this limit does not describe the numerical results.

The DMFT results are quite close to the static limit (12) only for the smallest frequency we considered, but they rapidly move away as the frequency rises, and already for $\omega_0 = 0.2D$ the difference between the calculation and the Fermi-liquid prediction becomes huge. This means that a standard Fermi-liquid approach can only be applied in the extremely adiabatic regime, and that even for small phonon frequencies, there are quantitatively important corrections to the theory.

As an attempt to provide a reference for the intermediate- ω_0 regime, we considered a “mixed limit” solution, in which the vertices Λ are taken as the geometric average between the two limiting expressions (12) and (13). As one can see in Fig. 6 this “mixed limit” solution has a behavior similar to the DMFT data. Interestingly, this heuristic choice has the advantage of staying finite for $n \rightarrow 1$, while the static limit goes to zero and appears to be appropriate only in the extremely small frequency limit.

IV. SCREENING OF COULOMB REPULSION BY PHONONS

Differently from the half-filled case, in the regimes considered in this paper we could not estimate U_{eff} from the quasiparticle weight Z since the delocalizing effect of the Coulomb screening turns out to be irrelevant. We can however discuss how the screening of Coulomb repulsion due to e-ph interaction influences the behavior of the chemical potential μ .

At half-filling μ is fixed by the particle-hole symmetry condition, while now, it needs to be determined in order to yield a given value of the density n .

In Fig. 7 we report μ vs λ as obtained within DMFT in the Hubbard-Holstein model varying the ratio ω_0/D , comparing, for $U = 5D$, the cases with $n = 0.30$, $n = 0.50$ and $n = 0.90$. For all densities μ decreases linearly in λ , while the role of ω_0 changes with the value of the density: for very small densities the slope of μ vs

λ monotonically decreases with increasing ω_0 while it increases for n close to 1 and it is practically constant in ω_0 at quarter filling ($n = 0.50$). Such a behavior of the chemical potential with n can be explained taking a closer look to the self-energy $\Sigma(i\omega_n)$. The real part of the self-energy at zero frequency shifts in fact the chemical potential in the interacting case according to $\mu = \mu_0 + \Sigma'(i\omega_n \rightarrow 0)$, leading to $\mu_\lambda = \mu_{\lambda=0} + \Sigma'_{res}(i\omega_n \rightarrow 0)$. A first indication on the behavior of $\Sigma(0)$ and μ can be derived through the Hartree-Fock (HF) approximation. In this light it is useful to formally integrate out the phononic degrees of

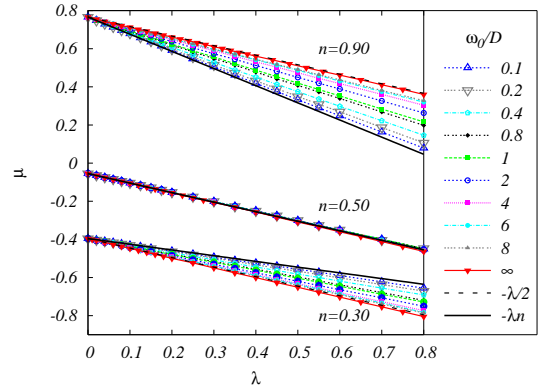


FIG. 7: (Color online) Behavior of the chemical potential as a function of λ for different values of ω_0/D . The cases of $n = 0.90$, $n = 0.50$ and $n = 0.30$, all obtained for $U = 5D$, are shown with the same scale. The full and dashed black lines are described below in the text.

freedom in Eq. (1). The result is a retarded phonon-mediated interaction

$$V(\omega) = -\lambda D \frac{\omega_0^2}{\omega_0^2 - \omega^2} \quad (14)$$

Including the Hubbard repulsion, the total interaction between electrons with opposite spin is then given by $U + 2V(\omega)$, while only $V(\omega)$ is present between electrons with parallel spin. The Hartree term equals $(U - 2\lambda D) \cdot n/2$. The interaction term $U + 2V(\omega)$ between electrons with spin σ and $-\sigma$ contributes in fact with $(U - \lambda D) \cdot n/2$ and the remaining $-\lambda D \cdot n/2$ comes from the term $V(\omega)$ between electrons with the same spin σ .

The equal-spin term gives also rise to a Fock diagram:

$$\Sigma_\sigma^{Fock}(i\omega_n) = -\frac{\lambda D}{2} \int dE N(E) \left(\frac{\omega_0}{i\omega_n - E - \omega_0} [f(E) + b(-\omega_0)] - \frac{\omega_0}{i\omega_n - E + \omega_0} [f(E) + b(\omega_0)] \right), \quad (15)$$

where f and b denotes respectively the Fermi and Bose functions, and $N(E)$ is the density of state per

spin. In the small- ω_0 limit this yields the well known $-\lambda D N(0) i\omega_n$ result,⁴⁴ and therefore the Hartree-Fock

(HF) self-energy at zero frequency is given by the Hartree term only, i.e.

$$\Sigma_{\sigma}^{HF}(0) = (U - 2\lambda D) \frac{n}{2} \quad (\omega_0 \rightarrow 0) \quad (16)$$

In the opposite limit, i.e. for $\omega_0 \rightarrow \infty$ keeping λ constant, it can be easily seen that Eq. (15) is equal to $\lambda D \cdot (n - 1)/2$, so that one obtains

$$\Sigma_{\sigma}^{HF}(0) = (U - \lambda D) \frac{n}{2} - \frac{\lambda D}{2} \quad (\omega_0 \rightarrow \infty) \quad (17)$$

It is quite obvious that the HF scheme is not expected to hold for the large values of the Hubbard repulsion ($U = 5D$), we are dealing with. For the pure Hubbard model it has indeed been found with iterated perturbation theory solution of the DMFT, that the Hartree-Fock U -dependence can be canceled by higher order contributions.^{45,46} This finding is confirmed by ED-DMFT of the pure Hubbard model, where the low frequency self-energy is almost independent on U for all $n < 1$.⁴⁷

Therefore we can expect that in the antiadiabatic limit, where the interaction is exactly a Hubbard one, the whole $U - \lambda D$ factor multiplying the density in the HF self-energy (see Eq. (17)), is equally counteracted by higher-order terms. This is confirmed by our results of Fig. 7, where $\mu(\lambda) - \mu_{\lambda=0} \simeq -\lambda D/2$ for all the considered densities in the antiadiabatic regime. This value is nothing but the constant term of Eq. (17), which survives the cancellation of the density-dependent term.

In the opposite adiabatic limit, we do not expect the phonon part of (16) to follow the same fate of the purely electronic one. In this regime, in fact, the phonon-mediated attraction is of completely different nature with respect to the instantaneous Hubbard repulsion and the terms containing λ , beyond the HF, are not forced to behave like the Hubbard term. In other words, while for large ω_0 the phonons induce a screening of the Coulomb repulsion leading to an effective repulsion $U_{eff} \simeq U - \lambda D$, at vanishing phonon frequency this effect is not present and $U_{eff} \simeq U$. On the basis of these considerations, in the limit $\omega_0/D \rightarrow 0$, we expect a cancellation only of the U -term in (16), leading to $\mu(\lambda) - \mu_{\lambda=0} \simeq -\lambda Dn$. Such a relation is confirmed by the DMFT data for small ω_0 and fits remarkably well with behavior obtained at all the considered values of the density, for the chemical potential (see the continuous line in Fig. 7). This also clarifies the origin of the opposite behavior displayed by μ for $n < 1/2$ and $n > 1/2$. In fact, as it can be seen still in Fig. 7, the fully antiadiabatic curve (denoted by $\omega_0 = \infty$),⁴⁸ lays below all the other ones for $n = 0.30$, contrary to the case of $n = 0.90$ in which it lays above. Moreover, still in Fig. 7 it can be seen that the chemical potential is almost completely independent on ω_0 for $n = 0.50$, which is precisely what is predicted by the above considerations at quarter filling. This supports our idea that the frequency dependence of the λ -contribution to μ reflects the frequency dependence of the Coulomb screening by phonons, even though we cannot put this

idea on a quantitative basis as we did instead near the Mott transition at half-filling.

V. CONCLUSIONS

In this paper we have studied the effects of the e-ph interaction on a strongly correlated metal for filling different from $n = 1$. Choosing a large value of U/D the quasiparticle properties of the system are mainly controlled by the electron-electron correlations and polaronic features only appear at values of e-ph coupling λ larger by at least a factor two than those in the absence of correlation. However, even if the effective e-ph coupling for quasiparticles is reduced by the large Hubbard repulsion, we have identified a strong influence of the phonon dynamics. The quasiparticle weight Z , which in DMFT is inversely proportional to the effective mass, becomes very small because of the localizing effect of the Hubbard repulsion but it is still substantially influenced by the value of the phonon frequency and displays an unusual isotope effect. Specifically, since Z depends non monotonically on ω_0 , the isotope coefficient of the effective mass changes sign. This change of sign is a strong deviation with respect to Migdal-Eliashberg theory, and it is not present in the half-filled system, except for peculiar situations close to the bipolaronic transition and for specific values of U/D .⁴⁰ The effective quasiparticle e-ph coupling is particularly reduced in the small phonon frequency limit. From this point of view our DMFT results bear similarities with a mean-field calculation based on slave bosons and a variational Lang-Firsov transformation.⁴⁹ In that approach one obtains near half-filling $Z/Z_{\lambda=0} \simeq 1 - 1.388(\omega_0/D)\lambda$ at large U/D and small ω_0/D . In the adiabatic limit this expression implies a vanishingly small λ_{eff} , while in our DMFT λ_{eff} remains finite for $\omega_0 \simeq 0$, as a result of the quantum fluctuations that are neglected in the mean-field calculation. These values of λ_{eff} are however quite smaller than the bare λ , in agreement with a Fermi liquid description in terms of renormalized e-ph vertices in the static limit. It is interesting to note that the same mean-field approach/citepaolo2 predicts at large U/D a critical value $\lambda_{pol} \simeq U_c/2D$ for polaron formation which is slightly larger than the adiabatic value $\lambda_{pol} \simeq 1.328$ which is found for spinless fermions in the half-filled Holstein model and somewhat smaller than our estimates $\lambda_{pol} \simeq 2 \div 2.5$ at $U = 5D$.⁵⁰ For a single hole in the t - J with $J \simeq t/3$ a much smaller $\lambda_{pol} \simeq 0.8$ is required to reach a polaronic behavior. This is understood in terms of the pre-localizing mechanism associated with the antiferromagnetic background.^{17,18,51}

Beside the neglect of antiferromagnetic order and spin correlations, our DMFT approach is limited by the inability to capture the k -dependence of the self-energy, and accordingly of the quasiparticle weight. This limitation does not allow us to describe the momentum dependence of the effective e-ph coupling that has been

proposed to be induced by strong correlations by various authors.^{19,20,21} The momentum dependence can be restored by means of cluster extensions of DMFT, such as the Cellular Dynamical Mean-Field Theory. It has already been shown that, for the purely electronic Hubbard model, a significant momentum dependence establishes when the Mott transition is approached already for small clusters such as a 2×2 plaquette.⁵²

A further crucial assumption of the present work is the Holstein form of the electron-phonon coupling term. Although this kind of description has been justified for the cuprates by explicit calculations starting from a full three-band model,⁵³ it must be noted that the symmetry of the electronic degrees of freedom which are coupled by phonons plays a very important role in the competition between the phonon-mediated attraction and the Coulomb repulsion. In a model for fullerenes, in fact, in which the electrons are mainly coupled to Jahn-Teller vibrations, it has been found that the attraction between

electrons is not screened by a strong local repulsion, giving rise to unexpected phenomena like high-temperature superconductivity driven by strong correlation.^{54,55,56} More specifically in those models, phonon-mediated superconductivity is enhanced by the strong correlations close to the Mott transition, due to the specific symmetry of the phonons, which couple with orbital and spin degrees of freedom, as opposed to the Holstein coupling with the electron density.

Acknowledgments

We acknowledge useful discussions with Paolo Barone, Sergio Ciuchi, Michele Fabrizio, Erik Koch, Marco Grilli, Olle Gunnarsson, Paola Paci, Roberto Raimondi, and Alessandro Toschi. This work has been financed by Miur PRIN Cofin 2003 and by CNR-INFM.

-
- ¹ L. Pintschovius and W. Reichardt, in *Neutron Scattering in Layered Copper-Oxide Superconductors*, edited by A. Furrer (Kluwer Academic, Dordrecht, 1998), vol. 20, p. 165.
 - ² L. Pintschovius and M. Braden, Phys. Rev. B **60**, R15039 (1999).
 - ³ R. J. McQueeney, Y. Petrov, T. Egami, M. Yethiraj, G. Shirane, and Y. Endoh, Phys. Rev. Lett. **82**, 628 (1999).
 - ⁴ M. d'Astuto, P. K. Mang, P. Giura, A. Shukla, P. Ghigna, A. Mirone, M. Braden, M. Greven, M. Krisch, and F. Sette, Phys. Rev. Lett. **88**, 167002 (2002).
 - ⁵ P. V. Bogdanov, A. Lanzara, S. A. Kellar, X. J. Zhou, E. D. Lu, W. J. Zheng, G. Gu, J.-I. Shimoyama, K. Kishio, H. Ikeda, R. Yoshizaki, Z. Hussain, and Z. X. Shen, Phys. Rev. Lett. **85**, 2581 (2000).
 - ⁶ A. Lanzara, P. V. Bogdanov, X. J. Zhou, S. A. Kellar, D. L. Feng, E. D. Lu, T. Yoshida, H. Eisaki, A. Fujimori, K. Kishio, J. -I. Shimoyama, T. Nodaa, S. Uchida, Z. Hussain, and Z. -X. Shen, Nature **412**, 510 (2001).
 - ⁷ X. J. Zhou, T. Yoshida, A. Lanzara, P. V. Bogdanov, S. A. Kellar, K. M. Shen, W. L. Yang, F. Ronning, T. Sasagawa, T. Kakeshita, T. Noda, H. Eisaki, S. Uchida, C. T. Lin, F. Zhou, J. W. Xiong, W. X. Ti, Z. X. Zhao, A. Fujimori, Z. Hussain, and Z. -X. Shen, Nature (London) **423**, 398 (2003).
 - ⁸ B. Batlogg, R. J. Cava, A. Jayaraman, R. B. van Dover, G. A. Kourouklis, S. Sunshine, D. W. Murphy, L. W. Rupp, H. S. Chen, A. White, K. T. Short, A. M. Muzsaj, and E. A. Rietman, Phys. Rev. Lett. **58**, 2333 (1987).
 - ⁹ J. P. Franck, J. Jung, M. A.-K. Mohamed, S. Gyga, and G. I. Sproule, Phys. Rev. B **44**, 5318 (1991).
 - ¹⁰ T. Schneider and H. Keller, Phys. Rev. Lett. **69**, 3374 (1992).
 - ¹¹ Guo-Meng Zhao, M. B. Hunt, H. Keller, and K. A. Müller, Nature (London) **385**, 236 (1997).
 - ¹² J. Hofer, K. Conder, T. Sasagawa, Guo-Meng Zhao, M. Willemin, H. Keller, and K. Kishio, Phys. Rev. Lett. **84**, 4192 (2000).
 - ¹³ R. Khasanov, A. Shengelaya, K. Conder, E. Morenzoni, I. M. Savic, and H. Keller, J. Phys.: Condens. Matter **15**, L17 (2003).
 - ¹⁴ R. Khasanov, D. G. Eshchenko, H. Luetkens, E. Morenzoni, T. Prokscha, A. Suter, N. Garifanov, M. Mali, J. Roos, K. Conder, and H. Keller, Phys. Rev. Lett. **92**, 057602 (2004).
 - ¹⁵ G. Wellein, H. Röder, and H. Fehske, Phys. Rev. B **53**, 9666 (1996).
 - ¹⁶ M. Capone, M. Grilli, and W. Stephan, Eur. Phys. J B **11**, 551 (1999).
 - ¹⁷ A. S. Mishchenko and N. Nagaosa, Phys. Rev. Lett. **93**, 036402 (2004).
 - ¹⁸ O. Rösch and O. Gunnarsson, Phys. Rev. Lett. **93**, 237001 (2004).
 - ¹⁹ Z. B. Huang, W. Hanke, E. Arrigoni, and D. J. Scalapino, Phys. Rev. B **68**, 220507(R) (2003).
 - ²⁰ E. Cappelluti, B. Cerruti, and L. Pietronero, Phys. Rev. B **69**, 161101(R) (2004).
 - ²¹ E. Koch and R. Zeyher, Phys. Rev. B **70**, 094510 (2004).
 - ²² M. Grilli and C. Castellani, Phys. Rev. B **50**, 16880 (1994).
 - ²³ M. Capone, G. Sangiovanni, C. Castellani, C. Di Castro, and M. Grilli, Phys. Rev. Lett. **92**, 106401 (2004).
 - ²⁴ Gun Sang Jeon, Tae-Ho Park, Jung Hoon Han, Hyun C. Lee, and Han-Yong Choi, Phys. Rev. B **70**, 125114 (2004).
 - ²⁵ W. Koller, D. Meyer, Y. Ōno, and A. C. Hewson, Europhys. Lett. **66**, 559 (2004).
 - ²⁶ G. Sangiovanni, M. Capone, C. Castellani, and M. Grilli, Phys. Rev. Lett. **94**, 026401 (2005).
 - ²⁷ A. Georges, G. Kotliar, W. Krauth, and M. J. Rozenberg, Rev. Mod. Phys. **68**, 13 (1996).
 - ²⁸ K. Schönhammer and O. Gunnarsson, Phys. Rev. B **30**, 3141 (1984).
 - ²⁹ A. C. Hewson and D. Meyer, J. Phys.: Condens. Matter **14**, 427 (2002).
 - ³⁰ M. Caffarel and W. Krauth, Phys. Rev. Lett. **72**, 1545 (1994).
 - ³¹ For large values of λ it is particularly useful to work with shifted phonon variables, i.e. with a e-ph coupling term of the form $-g \sum_i (n_i - \bar{n})(a_i + a_i^\dagger)$. This choice reduces

- the average number of phonons which otherwise increases linearly with λ .
- ³² M. Capone and S. Ciuchi, Phys. Rev. Lett. **91**, 186405 (2003).
 - ³³ A similar behavior of Z has also been found in the Hubbard-Holstein model for smaller values of U and smaller n in a recent DMFT calculation using Numerical Renormalization Group: W. Koller and A. C. Hewson and D. M. Edwards, Phys. Rev. Lett. **95**, 256401 (2005)..
 - ³⁴ Notice that $P(X)$ is defined as a groundstate property while Z is related to quasiparticle excitations so that in principle polaronic quasiparticles can also be present without a multimodal $P(X)$, as it indeed happens for a single hole in the t - J model.
 - ³⁵ In the spectral functions for large values of U , the shape of the metallic peak at the Fermi level is weakly affected by the e-ph interaction, while visible phonons satellites appear on top of the lower and upper Hubbard bands.
 - ³⁶ M. Capone, W. Stephan, and M. Grilli, Phys. Rev. B **56**, 4484 (1997).
 - ³⁷ S. Ciuchi, F. de Pasquale, S. Fratini, and D. Feinberg, Phys. Rev. B **56**, 4494 (1997).
 - ³⁸ M. Capone, S. Ciuchi, and C. Grimaldi, Europhys. Lett. **42**, 523 (1998).
 - ³⁹ P. Paci, M. Capone, E. Cappelluti, S. Ciuchi, C. Grimaldi, and L. Pietronero, Phys. Rev. Lett. **94**, 036406 (2005).
 - ⁴⁰ P. Paci, M. Capone, E. Cappelluti, S. Ciuchi, and C. Grimaldi (2005), preprint.
 - ⁴¹ An alternative view to reconcile the substantial isotope effect on the penetration depth with the above findings is attribute it to isotope effects on collective modes. See G. Seibold and M. Grilli, Phys. Rev. B **72**, 104519 (2005).
 - ⁴² G. Sangiovanni, Ph.D. thesis, University of Rome "La Sapienza" (2005), <http://padis.uniroma1.it>.
 - ⁴³ P. Nozières, *Theory of Interacting Fermi Systems* (W. A. Benjamin, New York, 1964).
 - ⁴⁴ A. A. Abrikosov, L. P. Gorkov, and I. E. Dzyaloshinski, *Methods of Quantum Field Theory in Statistical Physics* (Dover Publications, 1963).
 - ⁴⁵ H. Kajueter and G. Kotliar, Phys. Rev. Lett. **77**, 131 (1996).
 - ⁴⁶ M. Potthoff, T. Wegner, and W. Nolting, Phys. Rev. B **55**, 16132 (1997).
 - ⁴⁷ While for $n < 1$ and large U , both μ and $\text{Re}\Sigma_\sigma(0)$ are almost independent of U , the same two quantities are directly proportional to U for $n > 1$. In fact, the chemical potential of the metallic phase, in a Hubbard model with large U , is always close, or even within, to one of the two Hubbard bands and these are distant $U - 2D$ one another.
 - ⁴⁸ The antiadiabatic solution labeled by $\omega_0 = \infty$ is calculated by solving a pure Hubbard model with total repulsion $U - \lambda D$ and with chemical potential $\mu + \lambda D/2$.
 - ⁴⁹ P. Barone, R. Raimondi, M. Capone, and C. Castellani Phys. Rev. B **73**, 085120 (2006).
 - ⁵⁰ Notice that the mean-field estimate of Ref. 49 increases by decreasing U/D up to $\lambda_{pol} \simeq U_c/D$ near $U \simeq U_c$.
 - ⁵¹ It is worth to note that also the FL description would suggest a greater relevance of e-ph coupling in the AF phase because of the larger value $Z \simeq J/t$ of the quasiparticle weight with respect to the paramagnetic phase at small doping.
 - ⁵² M. Civelli, M. Capone, S. S. Kancharla, O. Parcollet, and G. Kotliar, Phys. Rev. Lett. **95**, 106402 (2004).
 - ⁵³ O. Rösch and O. Gunnarsson, Phys. Rev. Lett. **92**, 146403 (2004).
 - ⁵⁴ M. Capone, M. Fabrizio, C. Castellani, and E. Tosatti, Science **296**, 2364 (2002).
 - ⁵⁵ J. E. Han, O. Gunnarsson, and V. H. Crespi, Phys. Rev. Lett. **90**, 167006 (2003).
 - ⁵⁶ M. Capone, M. Fabrizio, C. Castellani, and E. Tosatti, Phys. Rev. Lett. **93**, 047001 (2004).